Effect of the Fiber Content and Plasticizer Type on the Rheological and Mechanical Properties of Poly(vinyl chloride)/Green Coconut Fiber Composites

Jean L. Leblanc,[1] Cristina R. G. Furtado,[2] Marcia C. A. M. Leite,[2] Leila L. Y. Visconte,[3] Ana M. F. de Souza[3]

[1]*Polymer Rheology and Processing, University P. M. Curie (Paris 6), Paris, France*
[2]*Instituto de Química, Universidade do Estado do Rio de Janeiro, Rio de Janeiro, Brazil*
[3]*Instituto de Macromoléculas Professora Eloisa Mano, Universidade Federal do Rio de Janeiro, Rio de Janeiro, Brazil*

Received 11 October 2006; accepted 19 December 2006
DOI 10.1002/app.26567
Published online 30 August 2007 in Wiley InterScience (www.interscience.wiley.com).

ABSTRACT: A series of poly(vinyl chloride) (PVC)/green coconut fiber (GCF) composites, with dioctyl phthalate (DOP) or thermoplastic polyurethane (TPU) as a plasticizer, were prepared by melt mixing. Their properties were studied in the molten state with an advanced nonlinear harmonic testing technique; in the solid state, the hardness and impact resistance were evaluated, and scanning electron microscopy was used for fractured surfaces. The effect of the fiber loading was investigated, as well as the role of the plasticizer. PVC–GCF composites are heterogeneous materials that, in the molten state, exhibit essentially a nonlinear viscoelastic character, in contrast to pure PVC, which has a linear viscoelastic region up to 50–60% strain. The complex modulus increases with the GCF content but in such a manner that the observed reinforcement is at best of hydrodynamic origin, without any specific chemical (i.e., permanent) interaction occurring between the polymer matrix and the fibers. As expected, PVC offers good wetting of GCFs, as reflected by the easy mixing and the rheological and mechanical properties. Fibers can be incorporated into PVC up to a 30% concentration without any problem, with the PVC/plasticizer ratio kept constant. Higher GCF levels could therefore be considered. Replacing DOP in part with TPU gives some benefit in terms of impact resistance, likely because of the viscoelastic nature of the latter and the associated energy absorption effects. J Appl Polym Sci 106: 3653–3665, 2007

Key words: composites; fibers; mechanical properties; poly (vinyl chloride) (PVC)

INTRODUCTION

Raw materials from renewable resources are receiving growing and substantial attention in the scientific literature and in industry. Composites made of thermoplastic polymers and cellulose–lignin products, such as wood flour or certain natural fibers, are nowadays commercially available in certain parts of the world, and most developments are essentially pragmatic with relatively little understanding of the many scientific and technical aspects offered by such products. The main reason for using cellulose fibers in plastic composites is to merge the desirable properties of each component, but the current literature essentially focuses on fiber dispersion problems and fiber–matrix compatibility. Practically, it has been found that high-fiber-content composites are of interest, essentially for cost reasons, but because of the high viscosity of the mixtures and other ill-documented rheological effects during processing, uncontrolled aggregation of fibers is difficult to avoid.

In Brazil, large quantities of dried green coconut fibers (GCFs) are potentially available for manufacturing composites with thermoplastics. By nature, GCFs are a mixture of a dark brown powder with millimeter-to-centimeter-long fibers, which have been found to resist mixing within a polypropylene matrix.[1] The work reported here concerns poly(vinyl chloride) (PVC) composites with various amounts of GCFs and is a sequel to a previous publication in which polypropylene–GCF composites were studied with a thorough description of GCFs. Contrary to polypropylene (for which a compatibilizing agent is essential for providing good wetting of the fibers by the molten polymer), PVC was expected to naturally wet the fibers because of its polar nature. The objectives of this work were to evaluate the effects of the amount of GCF and the plasticizer type on the rheological and mechanical properties. A number of techniques were used, addressing the materials in both

Correspondence to: J. L. Leblanc (jean.leblanc@ifoca.com or jleblanc@ccr.jussieu.fr)

Contract grant sponsor: Coordenação de aperfeiçoamento de pessoal de nivel superior-Comite Français d'evaluation de la cooperation universitaire et scientifique avec le Brésil.

the molten and solid states, and scanning electron microscopy (SEM) was also used to interpret the obtained results.

EXPERIMENTAL

Polymer and other compounding ingredients

The following materials were used:

- Solvic 258 RG, a standard suspension-grade PVC in a powder form, supplied by Solvay Indupa (São Paulo, Brazil). Its density was 1.39 g/cm^3.
- GCF from Projeto Coco Verde (Rio de Janeiro, Brazil).
- Dioctyl phthalate (DOP), a plasticizer supplied by Vulcan S.A. (Rio de Janeiro, Brazil).
- 80A15, a commercial grade thermoplastic polyurethane (TPU) supplied by COFADE (São Paulo, Brazil). Its weight-average and number-average molecular weights were 193,000 and 77,000, respectively.
- UBZ Barostab 770 RH, a stabilizer supplied by Vulcan S.A. Its density was 0.96 g/cm^3.

GCFs

GCF manufacturing process

GCFs were prepared through a sequence of operations, including laceration, predrying, milling, and drying. Then, they were size-classified by passage through a 40-mesh sifter. Before the mixtures were prepared with PVC, the fibers were air-dried for 24 h at 80°C and for at least 1 h at 110°C until the moisture content stabilized around 4 wt %.

Analyzing GCF

The green coconut particle size distribution was evaluated with a testing sieve shaker (Bertel Indústria Metalúrgica, Ltd.) with the following sieves: 4, 32, 60, and 200. Figure 1 shows the size distribution

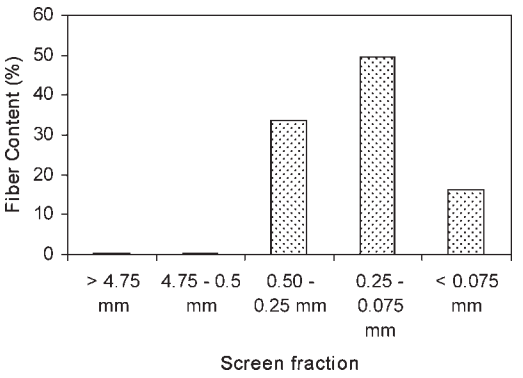

Figure 1 GCF size distribution.

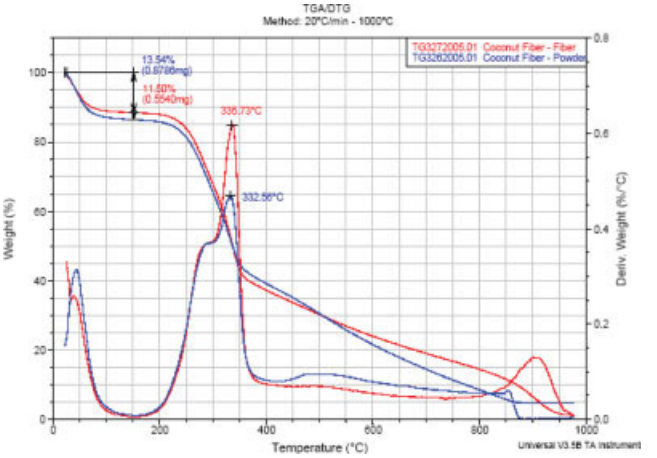

Figure 2 Thermogravimetric analysis of GCF powder and fiber. [Color figure can be viewed in the online issue, which is available at www.interscience.wiley.com.]

of the fibers. According to this analysis, the GCF sample used in this study was a mixture of long fibers and a fine powder. Most of the fibers (84%) were between 0.5 and 0.075 mm long, and the powder particle size (16%) was lower than 0.075 mm.

The densities of the fiber and powder were determined at room temperature with a glass pycnometer with ethanol. The tests were carried out in triplicate. The fiber and powder densities were 1.176 and 1.288 g/cm^3, respectively.

Thermogravimetric analysis/differential thermal analysis was performed on a TA Instrument TGA2050 thermal analyzer under nitrogen at a heating rate of 20°C/min. Figure 2 shows the thermogravimetric analysis of the GCF powder and fiber. On the basis of this analysis, the fibers and powder showed the same thermal behavior, and their moisture contents were 11.6 and 13.5%, respectively. Significant thermal degradation occurred above 200°C, and this indicated that safe mixing could be performed with PVC, whose processing temperature must generally remain below 180°C.

PVC–GCF composites

The experimental work reported here consisted of two parts: (1) a simple evaluation of the effects of the GCF loading on the properties of (slightly) plasticized PVC composites and (2) an evaluation of the effects of substituting the plasticizer with a thermoplastic urethane polymer. Part 2 was performed at a constant GCF loading. With respect to the preliminary works,[2,3] which demonstrated that the dry blending of the ingredients, followed by melt mixing in a Haake Rheocord 900 fixed with a 85-cm^3 mixing chamber with cam rotors, was the best method on the laboratory floor, all composite samples were prepared in this manner. Table I presents the formula-

TABLE I
PVC–GCF Composite Samples: Formulations and Preparation Procedures

Sample	PVC (g)[a]	GCF (g)[b]	DOP (g)[c]	UBZ (g)[d]	TPU (g)[e]
VCF00	100	—	10	4	—
VCF90	90	10	9	3.6	—
VCF80	80	20	8	3.2	—
VCF70	70	30	7	2.8	—
VCU70	70	30	7	2.8	—
VCU52	70	30	5	2.8	2
VCU34	70	30	3	2.8	4
VCU07	70	30	0	2.8	7

The preparation consisted of dry-blending the ingredients before loading a laboratory mixer. The starting temperature was 130°C, the fill factor was 0.70, the cam rotor speed was 50 rpm, the final torque was 17–19 Nm min, and the dump temperature was 158–160°C.

[a] Solvic 258RG, which was supplied by Solvay Indupa (Sao Paulo, Brazil).

[b] Supplied by Projeto Coco Verde S.A. (Rio de Janeiro, Brazil).

[c] Plasticizer.

[d] Antidegradant.

[e] 80A15 (Shore A hardness = 80), which was supplied by COFADE (São Paulo, Brazil).

tions of all the prepared samples. To have sufficient material for all the experimental techniques used, several preparation exercises were conducted for each formulation. The concentrations of the plasticizer (DOP) and the antidegradant (UBZ) were always 10 and 4 wt %, respectively, with respect to PVC. After mixing, the samples were compression-molded at 160°C and kept in plastic bags at room temperature. With respect to Table I, the reproducibility of the preparation technique was assessed by the consideration of samples VCF70 and VCU70 (three times the same formulation). Table II presents the composite formulations in terms of the volume fractions of the ingredients.

RESULTS AND DISCUSSION

Rheological data

Fourier transform (FT) rheometry: test protocols, data treatment, and analysis techniques

Like most other complex polymer systems, polymer–GCF composites are expected to exhibit a strong nonlinear viscoelastic character that needs special testing techniques to be studied. One such technique is FT rheometry, which was recently implemented by the suitable modification of commercial torsional dynamic rheometers.[4,5] Molten GCF composites are stiff (and heterogeneous) materials that cannot be conveniently tested with standard open-gap rheometers, such as cone-and-plate or parallel discs. A close-cavity torsional rheometer, such as the RPA 2000 rubber process analyzer (Alpha Technologies), has been proven recently to give reliable and reproducible results with PVC–GCF composites, provided that the appropriate sample handling technique is used.[3] Details on the modification of the RPA for FT rheometry have been published elsewhere,[6,7] as well as the calculation techniques to extract and analyze Fourier spectra from recorded strain and torque signals. FT rheometry finds its roots in large-amplitude oscillatory strain experiments, and because torque signals are resolved in all their components, this test technique is particularly well suited to any nonlinear response arising from the application of a large strain, from the fact that the tested material has an intrinsic nonlinear character (because of its complex morphology), or from both.

Through the experience gained in testing various different materials, test protocols were developed for nonlinear viscoelastic investigations, which essentially consist of performing strain sweep experiments through two subsequent runs separated by a resting period of 2 min after a warm-up period of 5 min 30 s (in fact, a first resting time in the closed cavity of 3 min followed by 0.2°, 1-Hz oscillations for 30 s and then another resting period of 2 min). At least two samples of the same material are tested (more if the results reveal gross test material heterogeneities) in such a manner that, through the inversion of the strain sequences (i.e., runs 1 and 2), sample fatigue effects are detected, if any. At each strain sweep step, 20 cycles are recorded, with an acquisition of 512 pt/s. FT calculations are consequently run with 2^{13} data points, which are sufficient for a good signal/noise ratio in such a manner that significant harmonics (if any) are detected up to the 15th one. Out of the FT treatment of the torque signal, one extracts essentially two types of information: first, the main torque component, that is, the peak in the FT spectrum that corresponds to the applied frequency (i.e., 1 Hz in this work), and second, the harmonics, with the third (i.e., the peak at 3 times the applied frequency) the most intense one. The FT treatment of the strain signal provides information about the

TABLE II
PVC–GCF Composite Samples: Volume Fractions

Sample	PVC	GCF	DOP	UBZ	TPU
VCF00	0.8335	—	0.1182	0.0483	—
VCF90	0.7509	0.0991	0.1065	0.0435	—
VCF80	0.6681	0.1984	0.0948	0.0387	—
VCF70	0.5852	0.2979	0.0830	0.0339	—
VCU70	0.5852	0.2979	0.0830	0.0339	—
VCU52	0.5872	0.2990	0.0595	0.0340	0.0202
VCU34	0.5893	0.3001	0.0358	0.0341	0.0406
VCU07	0.5925	0.3017	—	0.0343	0.0715

The specific gravities were as follows: PVC, 1.39 g/cm^3; GCF, 1.17 g/cm^3; DOP, 0.98 g/cm^3; UBZ, 0.96 g/cm^3; and TPU, 1.152 g/cm^3.

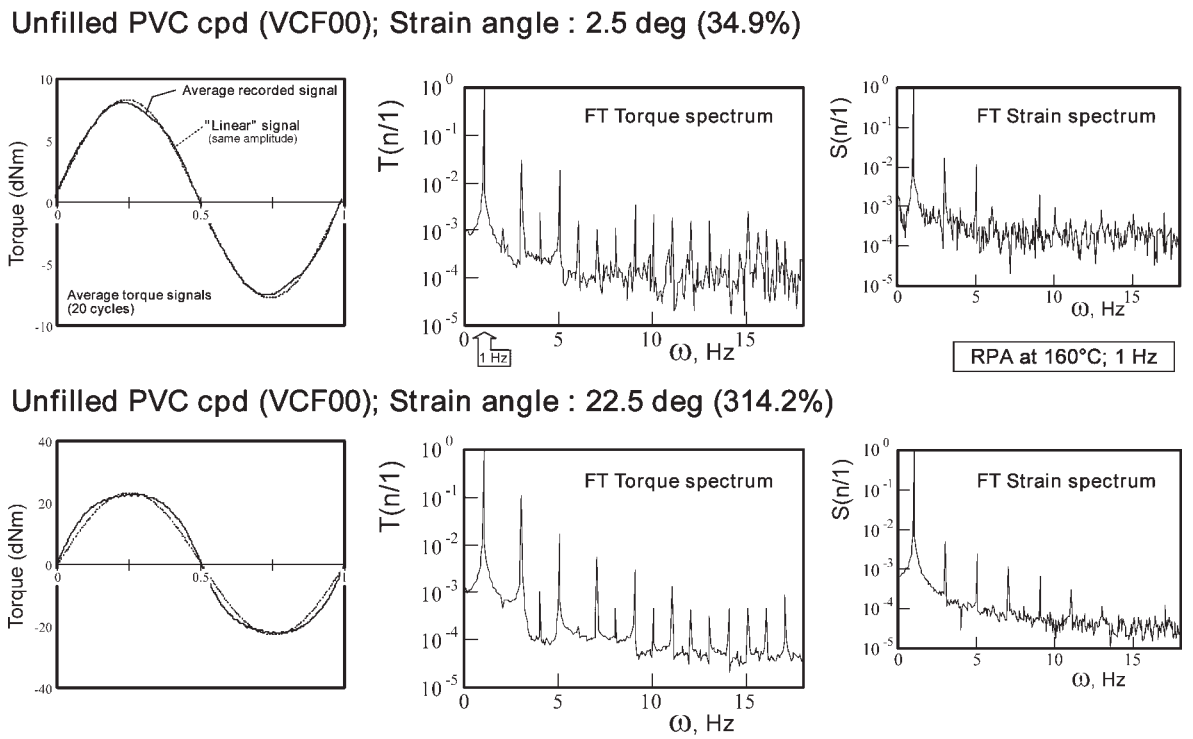

Figure 3 Typical results of FT rheometry for samples of unfilled PVC compounds at different strain amplitudes.

quality of the applied deformation and, as explained later, allows the correction of data for the technical limits of the instrument.

Preliminary experiments with PVC–GCF composites showed that some sample preparation is needed for reproducible results to be obtained, notwithstanding the intrinsic quality of the material. Disks around 5 cm in diameter were first cut out of 1.5–1.7-mm-thick molded plaques; then, through weighing, their volume was controlled to be within the RPA test cavity volume plus around 5% (i.e., 3.15 cm^3 with the 20-groove dies and the gap setting, i.e., 0.485 mm, used). All RPA–FT tests were conducted at 160°C, but it was found that using a starting temperature 20°C higher (when the cavity was closed) and then cooling down immediately toward the test temperature gave improved reproducibility with PVC–GCF composites because this technique ensured excellent filling of the cavity, with complete closure at the end of the warm-up period (i.e., 330 s) and thermal homogeneity of the sample.

Figure 3 shows typical results for a sample of an unfilled PVC compound at different strain amplitudes. The left graphs show the average torque signals of 20 recorded cycles; perfect sinusoids of the same amplitude are drawn for comparison. The middle graphs are the corresponding FT torque spectra. The right graphs are the FT spectra for the applied strain. One notes incidentally that, at a low strain, both the torque and strain spectra are noisier than at a higher strain. Ideal dynamic testing would require that a perfect sinusoidal deformation at a controlled frequency and strain be applied to the test material. This aspect is rarely considered in the literature, and the quality of the applied signal is generally taken for granted. Despite the quality design and care in manufacturing modern dynamic instruments, there are always technical limits in accurately submitting a test material to harmonic strain. As detailed elsewhere,[6] FT analysis reveals relatively significant (i.e., larger than noise) odd harmonic components in the RPA strain signal, with the third obviously the larger one, particularly at a low-strain amplitude. Whatever the test conditions are, the relative third harmonic strain component [$S(3/1)$] decreases as the strain amplitude increases and generally passes below 1% of the main component when a sufficient strain angle is reached, depending on the stiffness of the tested materials. In other words, high-strain tests are performed under better applied signal conditions than low-strain ones.

As shown in Figure 3, upon a strain amplitude of 22.5° (i.e., 314% strain), the torque signal is clearly distorted, and this corresponds to a nonlinear character well assessed by the FT spectrum with significant odd harmonics. However, at a lower strain (2.5°; 35%), a slight distortion is nevertheless noted and characterized also by odd harmonics, in agreement with the onset of strain dependence detected on the complex modulus (G^*; Fig. 4).

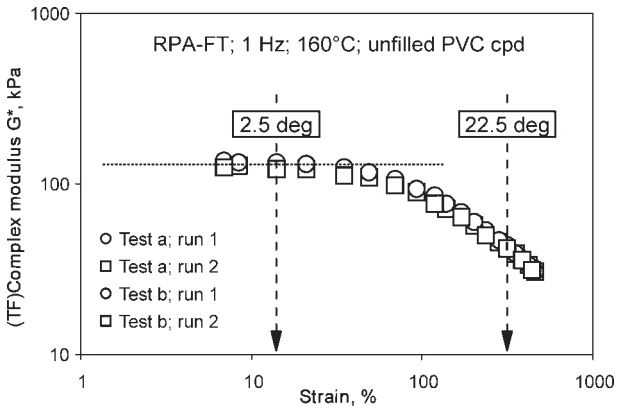

Figure 4 Typical strain sweep test of an unfilled PVC compound polymer.

With respect to Figure 4, standard harmonic testing would be limited to around 40% strain ($\approx 3^\circ$) for valid splitting of G^* into elastic and viscous components; otherwise, apparent (and meaningless) data would be obtained. FT rheometry is thus not limited to the linear response of polymer materials but allows the overall viscoelastic behavior to be investigated in detail.

The nonlinear response of the material is documented by odd harmonics detected in the torque signal, with the third the most intense one. As shown in the upper right graph of Figure 5, the (relative) third torque harmonic, as measured with the updated RPA, does not correspond to the theoretical expectation that harmonics vanish as the linear viscoelastic region is reached at a low strain. The (relative) third strain harmonic variation with the strain amplitude (lower left graph) suggests obviously that poor applied strain quality at a low amplitude is responsible for this artifact, which requires a correction.

A plot of the relative third torque harmonic component [$T(3/1)$] versus $S(3/1)$ suggests an adequate method to correct torque harmonic components for deficiencies in the applied strain (right upper graph of Fig. 3). Indeed, $T(3/1)$ versus $S(3/1)$ decreases, passes through a minimum, and appears to be bounded by a straight line whose slope is a multiple of 1/3. If an ideal elastic material, for instance, the calibration spring, is tested, then the slope is 2/3. The correction method is based on the simple argument that, if the applied strain perfect were perfect, all $T(3/1)$ data points would fall on the vertical axis.

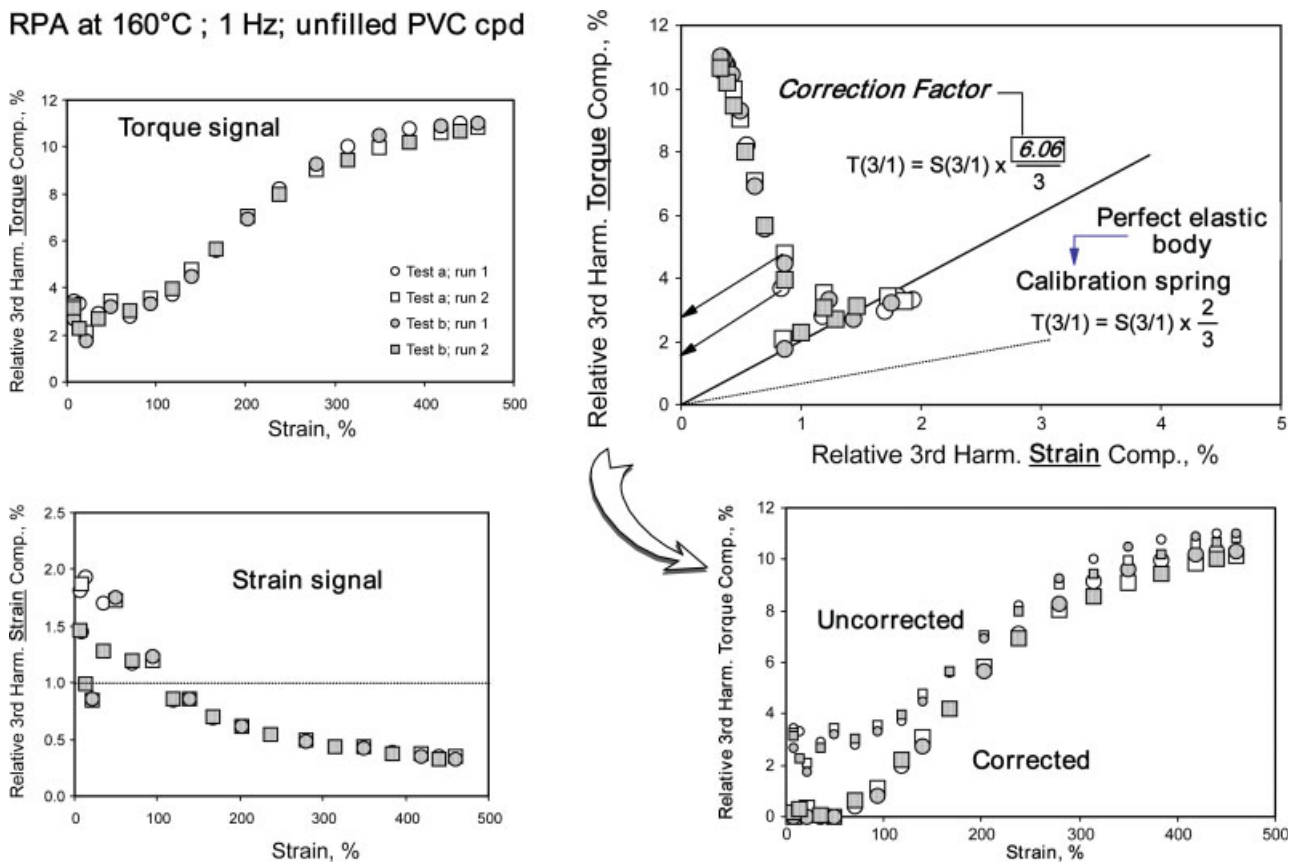

Figure 5 Torque and strain harmonics and correction method for the relative third torque component data: FT rheometry for an unfilled PVC compound.

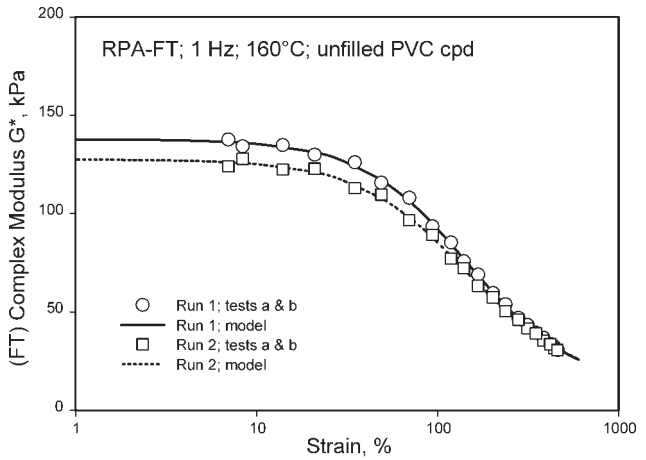

Figure 6 Variation of FT G^* with the strain amplitude for an unfilled PVC compound.

Consequently, the $T(3/1)$ data are corrected as follows:

$$T(3/1)_{\text{corr}} = T(3/1)_{TF} - S(3/1)_{TF} \times (\text{CF}/3) \qquad (1)$$

where $T(3/1)_{\text{corr}}$ is the corrected relative third torque harmonic component; $T(3/1)_{TF}$ and $S(3/1)_{TF}$ are the measured relative third harmonic components of the torque and strain signals, respectively; and CF is the correction factor derived from the $T(3/1)$–$S(3/1)$ plot. The lower right graph in Figure 3 shows how this correction method works well, with the immediate result that at a low strain, when the viscoelastic response of the material is expected to be linear, the correct relative third torque harmonic component vanishes, in agreement with theory.[4]

RPA–FT results, according to test protocols described previously, yield essentially two types of information, which reflects how the main torque, that is, $T(\omega)$, and the (corrected) relative third torque harmonic component, that is, $T(3\omega)/T(\omega)$ or $T(3/1)$, vary with the strain amplitude. At a low strain (and provided that the test material exhibits a linear response within the experimental strain window, i.e., between 0.5 and 33.0° at 1 Hz with the RPA), $T(\omega)$ shows a linear variation with the set strain (γ) and then deviates from linearity as nonlinearity develops. The ratio $T(\omega)/\gamma$ obviously has the meaning of a modulus, and for a material exhibiting linear viscoelasticity within the considered strain amplitude, one gets the most familiar picture of a plateau region at a low strain and then a typical strain dependence. FT yields the main torque component in arbitrary units, but with respect to the data acquisition conditions used for FT calculations, the following equality holds:

$$G^*(\text{kPa}) = 12.335 \times [T(\omega)/\gamma]$$

where $T(\omega)$ is measured in arbitrary units and γ is given as a percentage.

Figure 6 shows the FT G^* curve obtained when the strain sweep test protocol described previously is applied to an unfilled PVC compound. The reproducibility is correct, and there is a slight strain history effect (runs 1 and 2 do not superimpose). The G^* curve is adequately modeled with the following equation:

$$G^*(\gamma) = G_f^* + \{(G_0^* - G_f^*)/[1 + (A\gamma)^B]\} \qquad (2)$$

where G_0^* is the modulus in the linear region, G_f^* is the modulus for infinite strain, A is the reverse of a critical strain [which corresponds to $(G_0^* + G_f^*)/2$], and B is a parameter describing the strain sensitivity of the material. The so-derived linear modulus corresponds obviously to the initial slope of the $T(\omega)$–γ graph. A difference is seen between the data gathered through runs 1 and 2, thus demonstrating that the material is somewhat sensitive to the strain history or that any memory effect was not damped down during the 2-min dwelling time. Both G_0^* and G_f^* are extrapolated features and therefore have limited meaning, if any, when their numerical values are too far from measured data. With respect to Figure 6, G_0^* data would therefore be considered with confidence.

Figure 7 displays the $T(3/1)$–γ curve for an unfilled PVC compound. The data are well reproducible, with no differences between tests a and b and minor differences between runs 1 and 2. As previously reported,[5,6] the variation of $T(3/1)$ with the strain amplitude appears such that an S-shape curve is generally observed, from zero at a low strain up to a maximum at a high strain. According to theoretical considerations by Wilhelm et al.,[8] the upper limit of the relative torque harmonic $T(n\omega)/T(\omega)$ [or $T(n/1)$] should be expected to be equal to $1/n$. Indeed, despite the great variety of materials investi-

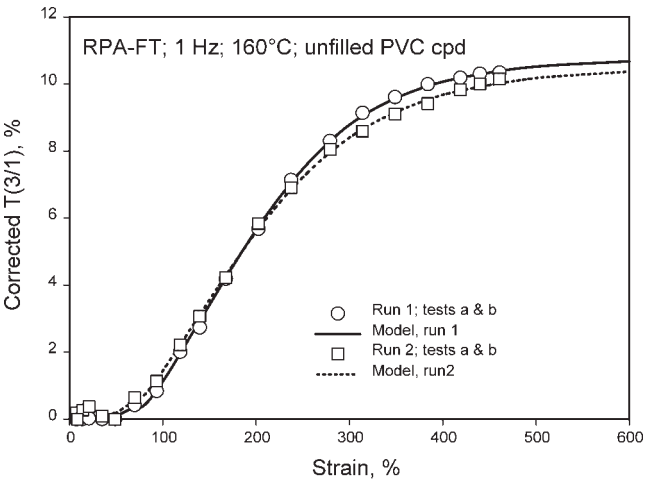

Figure 7 RPA–FT for an unfilled PVC compound: variation of $T(3/1)$ with the strain amplitude.

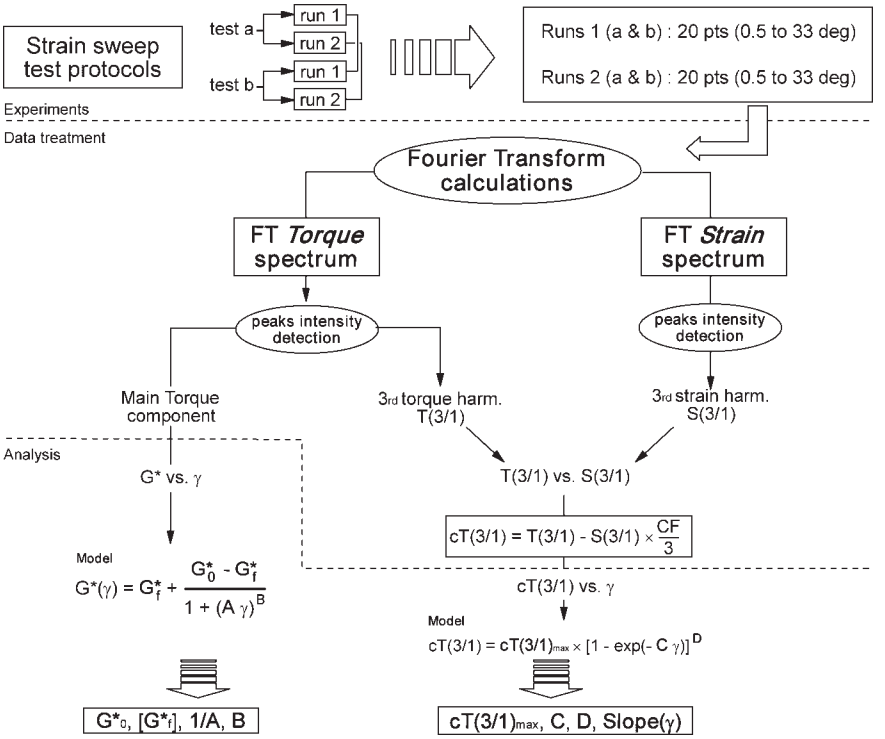

Figure 8 Synopsis of the RPA–FT experiments, data treatment, and analysis as applied to PVC–GCF composites.

gated so far, $T(3/1)$ higher than 33% has never been measured. Data in Figure 7 confirm these observations but clearly show that the occurrence of a plateau [$T(3/1)_{max}$] can be foreseen without doubt, with, however, a value significantly lower than 33%. The following model is used to fit $T(3/1)$–γ curves:

$$T(3/1)_{\gamma} = T(3/1)_{max} \times [1 - \exp(-C\gamma)]^{D} \qquad (3)$$

where $T(3/1)_{TF}$ is the relative third torque harmonic component depending on the deformation γ (%), and C and D are the fitting parameters. In terms of nonlinear viscoelastic behavior, the most significant information is provided by parameters C and D, which quantify the strain sensitivity of materials. The first derivative of eq. (3) allows the calculation of the slope of $T(3/1)$–γ curves at any strain; this is an easier way to quantify a strain effect than simultaneously considering C and D.

Figure 8 summarizes the RPA–FT experiments, data treatment, and analysis that were used in this work on PVC–GCF composites. The results consist of a set of single numbers that provide a full characterization of the linear and nonlinear viscoelastic behavior of materials in the molten state.

RPA–FT results on PVC–GCF composites in the molten state

Effects of the GCF loading. Figure 9 shows the typical G^* variation with the strain amplitude for the PVC–GCF composite with the highest GCF content. From a comparison with similar data for the unfilled PVC compound (Fig. 6), several key observations can be made. First, no plateau at a low strain is observed within the experimental window (i.e., 7–461%); in other words, the highly loaded PVC–GCF composite exhibits a strong nonlinear viscoelastic character. Second, there is a significant strain history effect, as the low-strain G^* drops by more than 100 kPa. Third, the difference between the run 1 and run 2 data vanishes at a high-strain amplitude.

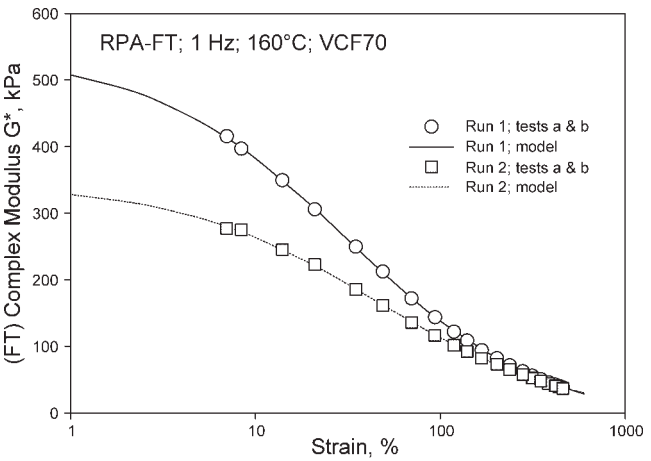

Figure 9 Variation of FT G^* with the strain amplitude for a PVC–GCF composite (Φ_{GCF} = 0.298).

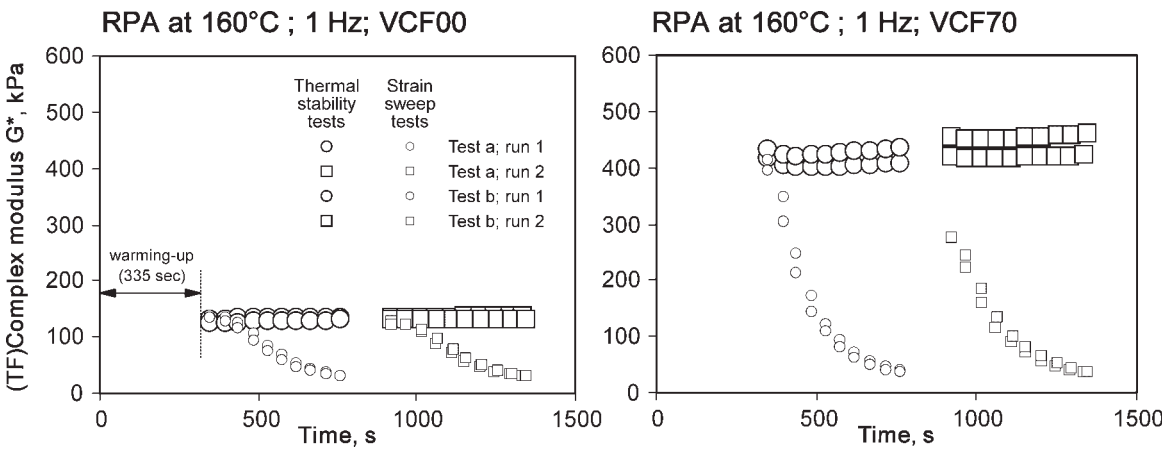

Figure 10 Thermal stability tests of an unfilled PVC compound and a PVC–GCF composite.

For complex polymer systems, the origin of the strain history effects is usually assigned to a heterogeneous morphology (or structure) that is destroyed, or at least modified, through large deformation. When two successive strain sweep tests are performed, according to the protocol previously described, the material is maintained in the RPA cavity at a high temperature for quite a long time (ca. 25 min). Therefore, thermal degradation of the materials cannot be excluded. To check this possibility, a so-called thermal stability test protocol (at 160°C) was designed, which consisted of first warming the material (5.5 min) and then running 10 low-strain tests (i.e., 1.0°) twice with an intermediary resting period of 2 min. Torque and strain signals were recorded, and FT calculations were performed in the usual manner. Figure 10 shows results for the unfilled PVC compound (VCF00) and the 0.298 GCF volume fraction composite (VCF70) with respect to a time-scale, which represents the time exposure to 160°C. Tests were repeated to take into account the sample quality. For the sake of comparison, strain sweep data were also drawn versus the time of exposure (small symbols).

With respect to Figure 10, it is clear that no significant thermal degradation occurs within 23–25 min of exposure to 160°C for the unfilled PVC compound or the PVC–GCF composite. For the unfilled compound, the mean G^* values are 135.5 ± 1.4 and 130.3 ± 2.7 kPa for tests a and b, respectively; for the composite, the values are 413.1 ± 8.2 (test a) and 444.0 ± 14.7 kPa (test b). In fact, a slight increase in G^* (at 1 Hz, 1°) is observed with the composite, and this is likely due to better closure of the test cavity as the experiment proceeds. This effect is marginal, however, being smaller than the test-to-test reproducibility (directly related to the sample quality) and anyway in the reverse direction of the strain history effect. Strain history effects observed on PVC–GCF composites can consequently be assigned to changes in the material morphology occurring during the first strain sequence (run 1) and not recovered during the 2-min rest period before the second strain sequence starts.

As expected, increasing the GCF content significantly enhances the nonlinear viscoelastic character

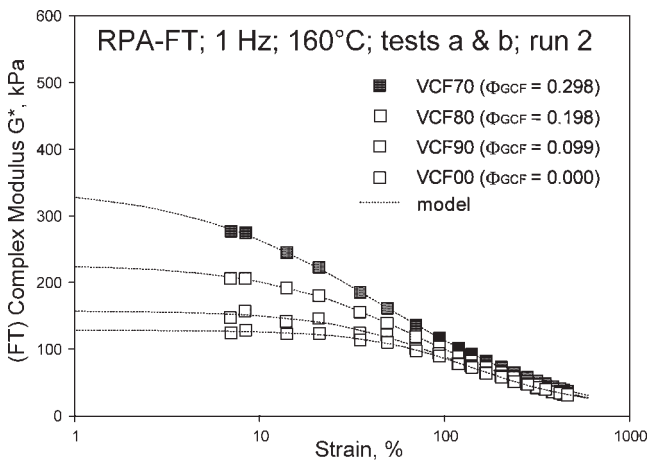

Figure 11 Effect of the GCF content on G^* versus the strain.

TABLE III
PVC–GCF Composites in the Molten State: Effects of the Fiber Loading on G^* Versus γ and the Fitting Parameters of Eq. (2)

Model		$G^*(\gamma) = G_f^* + \{(G_0^* - G_f^*)/[1 + (A\gamma)^B]\}$				
Sample	Run	G_0^* (kPa)	G_f^* (kPa)	$1/A$ (%)	B	r^2
VCF00	1	137.82	11.87	146.4129	1.48	0.9993
VCF00	2	127.56	12.93	145.3500	1.44	0.9987
VCF90	1	196.27	−5.37	110.5000	1.06	0.9851
VCF90	2	156.91	8.50	113.1200	1.21	0.9953
VCF80	1	312.08	−7.48	63.2500	0.95	0.9996
VCF80	2	226.40	1.43	77.1000	1.00	0.9998
VCF70	1	538.63	−16.46	31.2800	0.82	0.9999
VCF70	2	343.01	−8.59	45.4800	0.81	0.9998

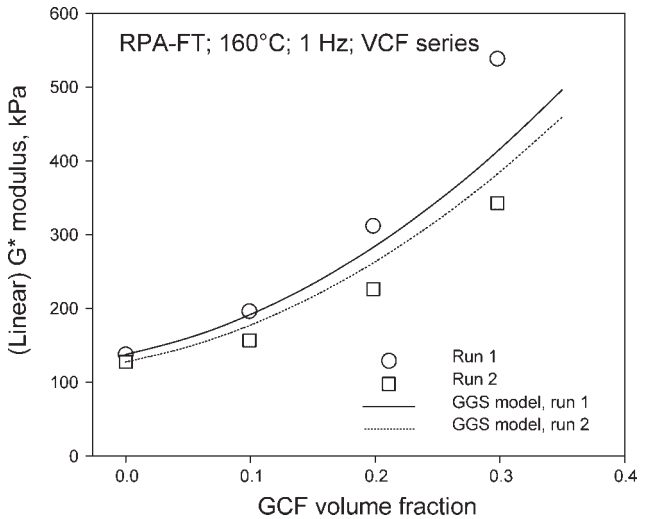

Figure 12 Effect of the filler loading on the extrapolated linear dynamic moduli of PVC–GCF composites. The plain and dashed lines were calculated with the Guth–Gold–Simha model.

of composites, as illustrated in Figure 11. How G^*–γ curves evolve with a higher GCF level validates the model expressed by eq. (2): as the fiber level increases, the linear plateau to lower limiting strains moves outside the experimental window of the rheometer when the fiber fraction is higher than 0.10. The (extrapolated) linear modulus (G_0^*), obtained during the fitting of the experimental data to eq. (2), can therefore be considered a true material parameter (Table III). On the contrary, G_f^* data must be considered mere fitting parameters, without any virtues other than those imparted by the fitting algorithm. As shown in Figure 11, all G^*–γ curves seem to converge at a high-strain amplitude, but the (expected) point of convergence is not in the experimental window. Negative G_f^* values have obviously no physical meaning, and the mean of all data (positive and negative) is -0.4. In other words, eq. (2) could be simplified by the omission of the G_f^* parameter. If this is done, however, the fit is generally of a lower quality

TABLE IV
PVC–GCF Composites in the Molten State: Effects of the Fiber Loading on $T(3/1)$ Versus γ and the Fitting Parameters of Eq. (3)

Model	$T(3/1)_\gamma = T(3/1)_{max} \times [1 - \exp(-C\gamma)]^D$				
Test	$T(3/1)_{max}$	C	D	r^2	Slope (200%)
VCF00, run 1	10.75	0.0112	5.72	0.9998	0.0431
VCF00, run 2	10.48	0.0100	4.33	0.9988	0.0378
VCF90, run 1	10.46	0.0129	4.68	0.9988	0.0358
VCF90, run 2	10.59	0.0108	3.74	0.9977	0.0353
VCF80, run 1	11.18	0.0140	3.66	0.9949	0.0295
VCF80, run 2	11.62	0.0102	2.71	0.9946	0.0329
VCF70, run 1	12.69	0.0135	2.19	0.9925	0.0232
VCF70, run 2	13.11	0.0097	1.86	0.9961	0.0297

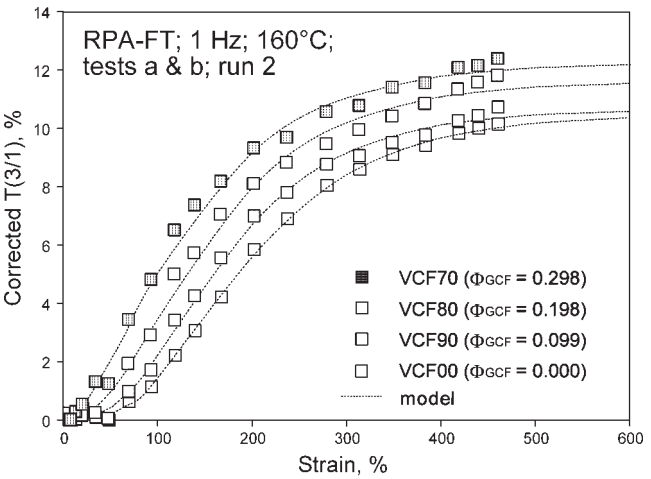

Figure 13 Corrected $T(3/1)$ versus γ for PVC–GCF composites. Two samples were tested (data for run 2).

because more statistical weight is then given to low-strain data.

G_0^* accounts for the net effect of the fiber loading, which is independent of the structural damages (or alterations) because of the amplitude of the applied strain. As shown in Figure 12, the reinforcing effect of GCFs and the strain history effect can be clearly seen when the linear modulus is plotted versus the fiber volume fraction. It is attractive to consider the GCF loading effect with respect to simple well-known models, such as the Guth–Gold–Simha equation:[9,10]

$$G_{cpd}^* = G_0^* \times (1 + 2.5\Phi + 14.1\Phi^2) \quad (4)$$

where G_{cpd}^* is the complex modulus of the compound, and Φ is the volume fraction of the filler.

The lines drawn in Figure 12 correspond to eq. (4) with G_0^* values of 137.82 (run 1) and 127.56 kPa (run

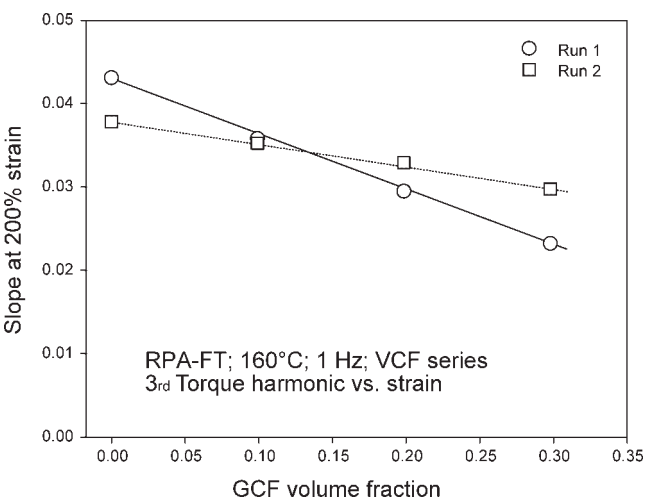

Figure 14 Relative third harmonic versus the strain for PVC–GCF composites. The slope was 200%.

TABLE V
PVC–GCF Composites in the Molten State: Effects of DOP Replacement by a TPU Polymer on G^* Versus γ and the Fitting Parameters for Eq. (2)

Model		$G^*(\gamma) = G_f^* + \{(G_0^* - G_f^*)/[1 + (A\gamma)^B]\}$				
Sample	Run	G_0^* (kPa)	G_f^* (kPa)	$1/A$ (%)	B	r^2
VCU70	1	582.42	8.45	45.66	0.99	1.0000
VCU70	2	415.73	3.74	52.44	0.93	0.9995
VCU52	1	689.50	9.12	45.17	1.02	0.9997
VCU52	2	479.46	2.20	52.03	0.97	0.9995
VCU34	1	786.96	10.14	46.13	1.06	0.9983
VCU34	2	547.03	5.12	49.80	0.97	0.9996
VCU07	1	909.12	16.54	50.97	1.07	0.9986
VCU07	2	709.29	5.53	49.80	1.00	0.9997

2), that is, the values for the unfilled PVC composition. The measured data for the PVC–GCF composites do not correspond to the model; the run 1 data are above it, and the run 2 data are below it. In developing their model, Guth, Gold, and Simha considered suspensions of noninteracting spheres of equal diameter, to which they assigned a purely hydrodynamic effect. Consequently, their model is expected to fail either when there are chemical or physicochemical interactions between the matrix and the dispersed phase or when the discrete phase content is high enough for particle–particle contacts to occur, as indeed reported by many authors. Conversely, one could consider that the closer to the model the experimental data are, the less probable polymer–filler interactions are. It follows that the data in Figure 12 strongly suggest that there is no significant permanent interaction between the PVC matrix and GCFs and that the high (extrapolated) modulus from run 1 data corresponds to initial contacts between fibers, which are easily disturbed by a mild strain. Run 2 data therefore describe the net reinforcing effect of GCFs.

Both the critical strain ($1/A$) and the strain sensitivity parameter (B) decrease linearly with higher values of Φ_{GCF} (volume fraction of green coconut fiber), without any significant difference between runs 1 and 2. This further documents the shrinking of the linear region as the fiber content increases, without any other meaning except that, as the polymer content decreases, the viscoelastic matrix has to support locally an increasing strain because of the higher stiffness of GCF.

Table IV reports the effect of the GCF content on $T(3/1)$, as expressed through the fitting parameters of eq. (3). As illustrated in Figure 13, (corrected) $T(3/1)$–strain curves nicely demonstrate how the viscoelastic character is affected by the fiber content. The quasi-disappearance of any linear response at a low strain is reflected by the rapid increase in the torque harmonics as Φ_{GCF} increases. The associated higher strain sensitivity is well quantified by the slope calculated near the mid-strain range (here at 200%). The slope at 200% varies linearly with the fiber level, but as shown in Figure 14, there is a significant difference between the run 1 and run 2 data, which exhibit different slopes with a pivot point that seems to coincide with the theoretical percolation level ($\approx$ 0.12–0.13).

Effects of the TPU polymer. Substituting the DOP plasticizer with the TPU polymer on a weight-to-weight basis has clear effects on the strain sensitivity of G^*, as reflected by the fitting parameters of eq. (2) (Table V). No negative G_f^* values are obtained, and the differences in the other fitting parameters are quite consistent with the G^*–γ graphs (Fig. 15). Again, the G^* variation can be seen as essentially resulting from the decrease in the DOP plasticizer content (concomitant with the increase in the TPU level). However, the specific gravities of DOP and TPU differ significantly (DOP, 0.98 g/cm^3, and TPU, 1.152 g/cm^3),

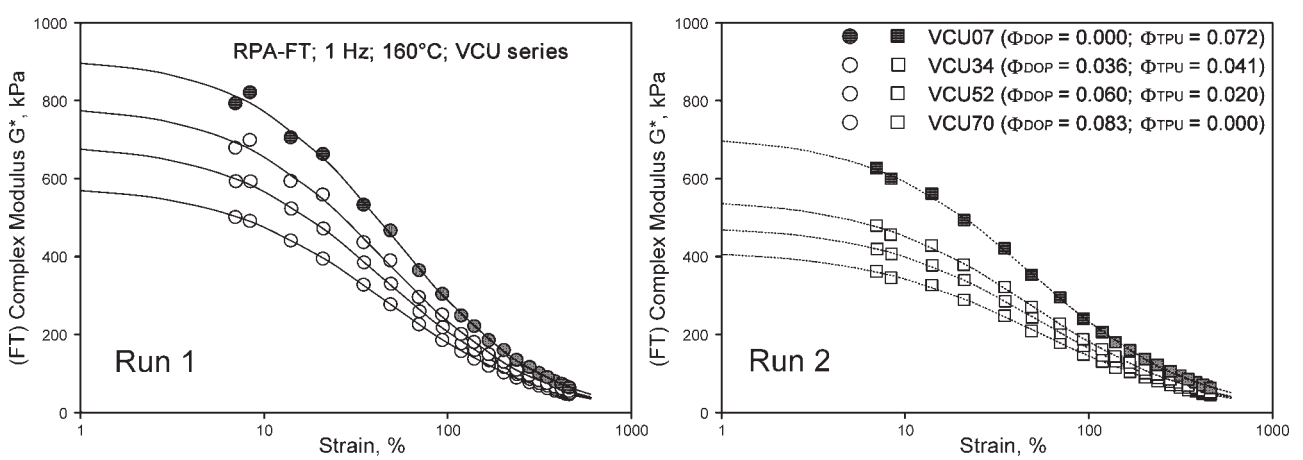

Figure 15 Effect of substituting the DOP plasticizer with the TPU polymer on G^* versus the strain for PVC–GCF composites in the molten state.

TABLE VI
PVC–GCF Composites in the Molten State: Effects of DOP Replacement by a TPU Polymer on *T*(3/1) Versus γ and the Fitting Parameters for Eq. (3)

Model Test	$T(3/1)_\gamma = T(3/1)_{max} \times [1 - \exp(-C\gamma)]^D$				
	$T(3/1)_{max}$	C	D	r^2	Slope (200%)
VCU70, run 1	12.22	0.0140	3.09	0.9911	0.0282
VCU70, run 2	12.73	0.0103	2.39	0.9934	0.0330
VCU52, run 1	12.27	0.0142	3.22	0.9900	0.0287
VCU52, run 2	12.73	0.0109	2.61	0.9934	0.0337
VCU34, run 1	12.39	0.0142	3.32	0.9908	0.0297
VCU34, run 2	12.68	0.0121	2.85	0.9926	0.0327
VCU07, run 1	12.62	0.0137	3.37	0.9967	0.0321
VCU07, run 2	13.52	0.0145	3.55	0.9975	0.0331

and so replacing the former with the latter on a weight-to-weight basis results in fact in (slightly) increasing GCF content (see the volume fractions in Table II).

The effects of substituting DOP with the TPU polymer on the third torque harmonics are given in Table VI in terms of the fitting parameters of eq. (3). Marginal effects are observed when DOP is substituted by the TPU polymer, in terms of either the recalculated value at 200% strain of the relative third torque harmonic component ($T(3/1)_{200\%}$) or the slope at 200% strain. This suggests again good compatibility between PVC and TPU.

Mechanical data

Effects of the GCF loading

Figure 16 illustrates the effect of the fiber content (0, 10, 20, and 30 wt %) on the impact properties of PVC–GCF composites.

According to the literature, short fibers have a high specific area, and if they are homogeneously distributed, the fiber–matrix compatibility is expected to be improved. Moreover, the effect of short fibers on the impact strength is not easy to predict as that on the tensile strength, and the effect is sometimes positive and sometimes negative.[11,12] In this work, the impact strength of the reinforced composites

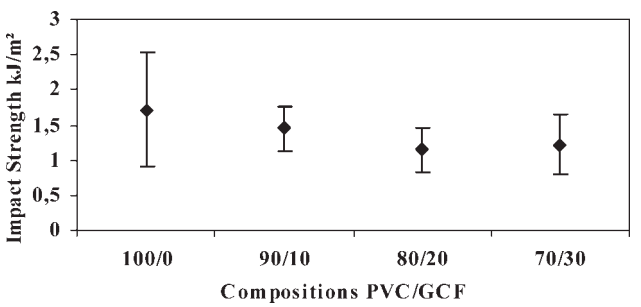

Figure 16 Impact strength of PVC and its composites as a function of the fiber content (95% confidence interval for the mean).

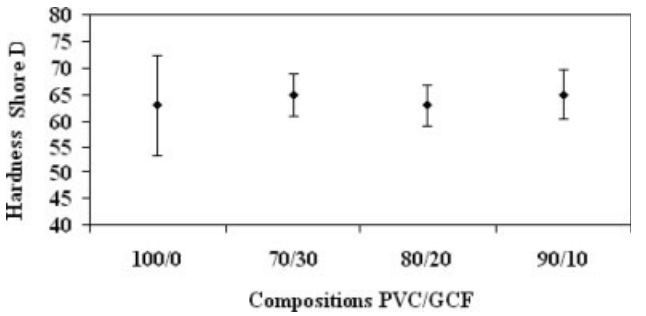

Figure 17 Shore D hardness of PVC and its composites as a function of the fiber content (95% confidence interval for the mean).

does not change much in comparison with that of unfilled PVC, whereas the results suggest a likely slightly beneficial effect of GCF concentrations greater than 30%. The same behavior is noted with the hardness because all the composites present similar values, as shown in Figure 17.

Effects of the TPU polymer

Generally, two types of plasticizers can be added to PVC compositions: a primary plasticizer, such as DOP, and a secondary one, which can be a polymer. In this work, TPU was used as a secondary plasticizer.

Figure 18 shows the effect of the plasticizer type (DOP or TPU) on the impact strength at a constant fiber content (30 wt %). VCU70 contains only 7% DOP; VCU07 contains no DOP but only 7% TPU. VCU52 and VCU34 are mixed plasticizer compositions. Increasing the TPU content, with some DOP still present in the formulation, significantly increases the impact strength. This behavior can be attributed to the elastomeric nature of TPU, which generates better impact properties, likely through the local dissipation of the impact energy, but because some DOP must be present, it is believed that internal plasticization of PVC is nevertheless needed.

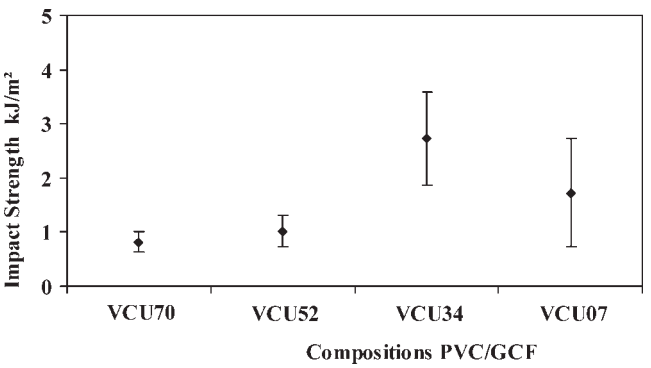

Figure 18 Impact strength of PVC–GCF composites as a function of the plasticizer type (95% confidence interval for the mean).

Morphology of the PVC–GCF composites

Figure 19 shows (liquid-nitrogen) fracture surfaces (SEM micrographs) of PVC/GCF/DOP composites. As expected, the higher the fiber content is, the larger the quantities are of fibers pulled out of the matrix during fracture. This suggests that, if indeed good wetting occurs between fibers and PVC (as suggested by FT rheometry results), this does not mean that permanent chemical interactions occur.

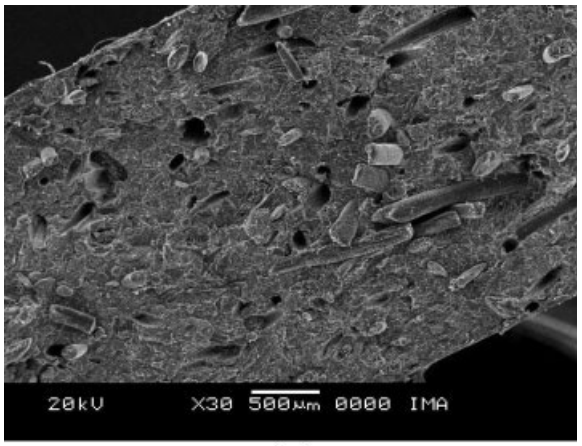

(a)

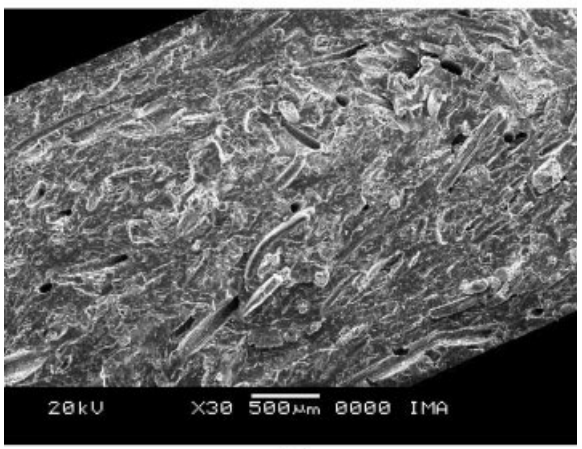

(b)

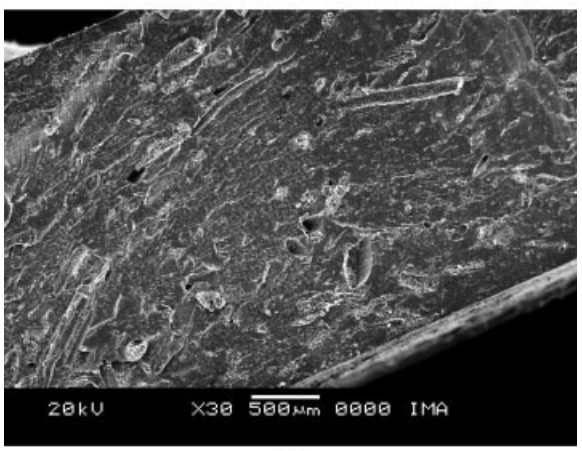

(c)

Figure 19 SEM photomicrographs of PVC–GCF composites with DOP as a plasticizer: (a) VCF70, (b) VCF80, and (c) VCF90.

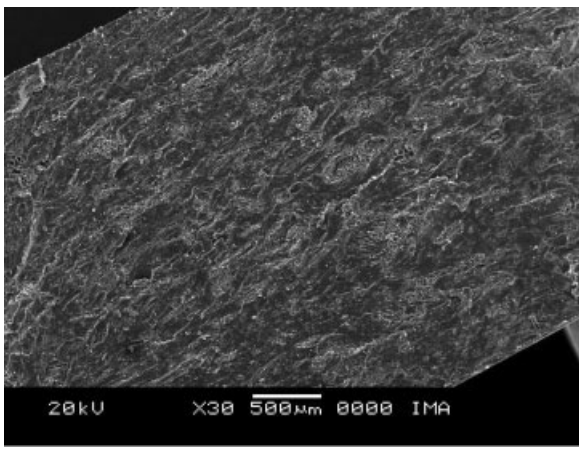

Figure 20 SEM photomicrograph of a PVC–GCF composite with TPU as a plasticizer (VCU07).

When TPU is used as a plasticizer in PVC compositions, one can nevertheless observe an increase in the fiber adhesion, as can be seen from a comparison of Figures 19(a) and 20. This can likely be explained by the higher viscosity imparted by the higher molecular weight TPU in comparison with DOP. This higher viscosity would favor a better incorporation of the fiber into the PVC matrix. Such observations are in line with both the rheological and impact properties.

CONCLUSIONS

On the basis of the experimental results, the following conclusions can be drawn:

1. PVC/GCF composites in the molten state exhibit nonlinear viscoelastic properties that are precisely and accurately documented through FT rheometry experiments. A net reinforcing effect is observed when GCFs are added in increasing quantities to PVC, but the effect is essentially hydrodynamic at a low fiber level and likely involves a structuration due to touching fibers at higher contents; strain history effects support this conclusion.
2. Impact and hardness properties are not significantly affected by the GCF content, and it follows that interesting composites can be prepared with up to 30% fiber without substantial changes in the mechanical (solid-state) properties.
3. Subtle effects are observed when some of the internal plasticizer, that is, DOP, is substituted by TPU; better fiber wetting is observed through

both rheological and mechanical properties and is well confirmed by an SEM morphological analysis.

This work was performed within the framework of a project sponsored by CAPES-COFECUB to promote collaboration between the University P. M. Curie (Paris 6) and the Universidade Federal do Rio de Janeiro. The authors express their thanks to Solvay Indupa (São Paulo, Brazil), Vulcan S.A. (Rio de Janeiro, Brazil), COFADE (São Paulo, Brazil), and Projeto Coco Verde S.A. (Rio de Janeiro, Brazil) for supplying the materials used in this work.

References

1. Leblanc, J. L.; Furtado, C. R. G.; Leite, M. C. A. M.; Visconte, L. L. Y.; Ishizaki, M. H. J Appl Polym Sci 2006, 102, 1922.
2. Ferreira, R. L.; Furtado, C. R. G.; Rosa, M. F.; Visconte, L. L. Y.; Follain, N.; Leblanc, J. L. Presented at the 5th International Symposium on Natural Polymers and Composites, São Pedro, Brazil, Sept 12–15, 2004.
3. Follain, N.; Leblanc, J. L.; Furtado, C. R. G.; Visconte, L. Y. Presented at the IUPAC World Polymer Congress, Macro 2004, Paris, France, July 4–9, 2004; Paper P4.3–6.9.
4. Wilhelm, M. Macromol Mater Eng 2002, 287, 83.
5. Leblanc, J. L.; de la Chapelle, C. Rubber Chem Technol 2003, 76, 287.
6. Leblanc, J. L. J Appl Polym Sci 2003, 89, 1101.
7. Leblanc, J. L. J Appl Polym Sci 2006, 100, 5102.
8. Wilhelm, M.; Reinheimer, P.; Ortseifer, M.; Neidhöfer, T.; Spiess, H. W. Rheol Acta 2000, 39, 241.
9. Guth, E.; Simha, R. Kolloid-Z 1936, 74, 266.
10. Guth, E.; Gold, O. Phys Rev 1938, 53, 322.
11. Carashi, J. C.; Ramos, U. M.; Leão, A. L. Acta Scientiarum 2002, 24, 1609.
12. van der Vegt, A. K. From Polymers to Plastic (Chapter 9)—VSSD, http://www.vssd.nL/hlf/m008.htm (accessed 2005).